

12-27-2017

Texture development and coercivity enhancement in cast alnico 9 magnets

Wenyong Zhang

University of Nebraska - Lincoln, wenyong.zhang@unl.edu

Shah Valloppilly

University of Nebraska-Lincoln

Xingzhong Li

University of Nebraska-Lincoln, xli2@unl.edu

Lanping Yue


University of Nebraska-Lincoln

Ralph Skomski

University of Nebraska-Lincoln, rskomski2@unl.edu

See next page for additional authors

Follow this and additional works at: <http://digitalcommons.unl.edu/cmrafacpub>

 Part of the [Atomic, Molecular and Optical Physics Commons](#), [Condensed Matter Physics Commons](#), [Engineering Physics Commons](#), and the [Other Physics Commons](#)

Zhang, Wenyong; Valloppilly, Shah; Li, Xingzhong; Yue, Lanping; Skomski, Ralph; Anderson, Iver; Kramer, Matthew; Tang, Wei; Shield, Jeff; and Sellmyer, David J., "Texture development and coercivity enhancement in cast alnico 9 magnets" (2017). *Faculty Publications from Nebraska Center for Materials and Nanoscience*. 129.
<http://digitalcommons.unl.edu/cmrafacpub/129>

This Article is brought to you for free and open access by the Materials and Nanoscience, Nebraska Center for (NCMN) at DigitalCommons@University of Nebraska - Lincoln. It has been accepted for inclusion in Faculty Publications from Nebraska Center for Materials and Nanoscience by an authorized administrator of DigitalCommons@University of Nebraska - Lincoln.

Authors

Wenyong Zhang, Shah Valloppilly, Xingzhong Li, Lanping Yue, Ralph Skomski, Iver Anderson, Matthew Kramer, Wei Tang, Jeff Shield, and David J. Sellmyer

Texture development and coercivity enhancement in cast alnico 9 magnets

Wenyong Zhang,^{1,2,a} Shah Valloppilly,² Xingzhong Li,² Lanping Yue,²
Ralph Skomski,^{1,2} Iver Anderson,³ Matthew Kramer,³ Wei Tang,³
Jeff Shield,^{2,4} and David J. Sellmyer^{1,2}

¹Department of Physics and Astronomy, University of Nebraska, Lincoln, NE 68588, USA

²Nebraska Center for Materials and Nanoscience (NCMN), University of Nebraska, Lincoln, NE 68588, USA

³Ames Lab, Iowa State University, Ames, IA 50011, USA

⁴Department of Mechanical and Materials Engineering, University of Nebraska, Lincoln, NE 68588, USA

(Presented 8 November 2017; received 30 September 2017; accepted 9 November 2017; published online 27 December 2017)

The effect of Y addition and magnetic field on texture and magnetic properties of arc-melted alnico 9 magnets has been investigated. Small additions of Y (1.5 wt.%) develop a (200) texture for the arc-melted alnico 9 magnet. Such a texture is hard to form in cast samples. To achieve this goal, we set up a high-field annealing system with a maximum operation temperature of 1250 °C. This system enabled annealing in a field of 45 kOe with subsequent draw annealing for the solutionized buttons; we have been able to substantially increase remanence ratio and coercivity, from 0.70 and 1200 Oe for the Y-free alnico 9 to 0.90 and 1400 Oe for the Y-doped alnico 9, respectively. A high energy product of 7.3 MGOe has been achieved for the fully heat-treated Y-doped alnico 9. The enhancement of coercivity is believed to arise from the introduction of magnetocrystalline anisotropy from 80 nm Y₂Co₁₇-type grains, which are exchange-coupled to the main-phase alnico rods. © 2017 Author(s). All article content, except where otherwise noted, is licensed under a Creative Commons Attribution (CC BY) license (<http://creativecommons.org/licenses/by/4.0/>). <https://doi.org/10.1063/1.5007171>

Alnico magnets, which consist of high-moment FeCo-rich and low-moment NiAl-rich phases, have many specific applications such as traveling-wave tubes, coin acceptors, and guitar pickups. They combine a high saturation magnetization, a very low temperature coefficient of magnetization, strong corrosion resistance, good machinability, and fairly low material costs. Their coercivities mainly arise from shape anisotropy, which is almost equal to $0.5J_s < 10$ kOe (J_s is the saturation polarization of the FeCo-rich phase). Therefore, the coercivity of alnico material is usually smaller than 2 kOe. Many efforts have been made to improve the hard-magnetic performance of alnico magnets by optimizing their nanostructure.¹⁻⁴ In order to increase coercivity, extra anisotropy such as magnetocrystalline anisotropy (often 1 to 2 orders of magnitude larger than shape anisotropy) may be needed.

Recently, it was reported that magnetocrystalline anisotropy can be introduced to alnico materials by forming a secondary noncubic phase, which helps to generate coercivity.⁵ These results prompted us to add rare-earth (RE) elements, which often react with Co and form RE-Co compounds with high magnetocrystalline anisotropy. Ti addition is necessary for obtaining large coercivity of alnico magnets. However, it restrains the formation of (200) texture, which is harmful for magnetic properties. Due to the limitation of elastic energy, spinodal decomposition takes place along $<100>$ directions of the mother alloy grain. Therefore, (100) texture favors the generation of preferred orientation of the FeCo-rich nanorods and the magnetic property enhancement. Kassen *et al.* used uniaxial

^awenyong.zhang@unl.edu

stress to promote the formation of near (100) texture in sintered alnico magnets from gas-atomized powders and to improve the magnetic performance.⁶ Tang *et al.* employed compression molding and subsequent sintering to induce the generation of near (100) preferred orientation and increase the energy product of the alnico magnets.⁷ Our recent experimental results show that, among the added RE elements (Sm, Dy, La, Pr, Y), Yttrium is effective because it not only introduces magnetocrystalline anisotropy in alnicos but also develops (100) texture. Thus we focus on the Y-added buttons.

The focus of this paper is on magnetic-field annealing, which will enhance the degree of the preferred orientation of the FeCo-rich nanorods, elongate the nanorods, increase the shape anisotropy field, and improve the squareness of hysteresis loops. Higher applied field for annealing ideally leads to stronger preferred orientation of the FeCo-rich phase, higher remanence ratios and energy products. So far, the applied maximum field for annealing is about 10 kOe. In order to further improve the magnetic properties of alnico magnets, the NCMN designed and installed an advanced high-field annealing system, whose maximum magnetic field and temperature are 45 kOe and 1250 °C, respectively. Specifically, we investigate the effect of Y addition and applied field on structure and magnetism of arc-melted alnico magnets.

10g buttons of $\text{Fe}_{35}\text{Co}_{35}\text{Ni}_{14.9}\text{Al}_{7.1}\text{Cu}_3\text{Ti}_5$, $\text{Fe}_{34.25}\text{Co}_{34.25}\text{Ni}_{14.9}\text{Al}_{7.1}\text{Cu}_3\text{Ti}_5\text{Y}_{1.5}$ were arc melted from high-purity elements in an argon atmosphere. The cylinders of 3 mm diameter and 7 mm length were made along the thickness direction of the buttons by an electro-discharge machine. The middle part was chosen for structure and property characterization. The cylinders were sealed in quartz tubes and solutionized at 1220 °C for one half hour followed by water quenching. They were then annealed in a high-field annealing furnace, pumped to a base pressure of 8×10^{-8} Torr at 800-840 °C for 10 min in a field of 45 kOe. In our experiments, the optimum spinodal decomposition temperature is 810 °C. Then draw annealing was done at 660 °C for 3 h and at 580 °C for 6 h. The phase composition was examined by Rigaku D/Max-B x-ray diffraction (XRD) with Co K_α radiation, and a Rietveld analysis of the x-ray diffraction patterns was performed using TOPAS software. The high-angle annular dark field (HAADF) imaging and element mapping were done with an FEI Tecnai Osiris (scanning) transmission-electron microscope (S/TEM). Electron diffraction patterns were simulated using software SAED2.^{8,9} The hysteresis loops and thermomagnetic curves were measured with a Quantum Design Physical Property Measurement System (PPMS) and a vibration sample magnetometer at fields up to 70 kOe. The field was applied parallel to the <200> direction of the buttons.

Figure 1 shows XRD patterns of Y-free, Y-added, and button powders solutionized at 1220 °C for one half hour and annealed at 810 °C for 10 minutes followed by draw annealing. All the samples mainly consist of the FeCo-rich and NiAl-rich phases. The lattice parameter a and concentration of the FeCo-rich and NiAl-rich phases for the Y-free button are 2.85 Å (55.4 wt%), 5.81 Å (44.6 wt%), respectively. They are 2.86 Å (48.3 wt%), 5.82 Å (36.7 wt%), respectively, for the Y-added button. The lattice parameters for the Y_2TM_{17} (15 wt%) phase are $a = 8.36$ Å and $c = 8.15$ Å close to the reported value.^{10,11} The lattice parameters of the FeCo- and NiAl-rich phases remain almost unchanged on Y addition, indicating that Y atoms didn't enter the FeCo- and NiAl-rich phase

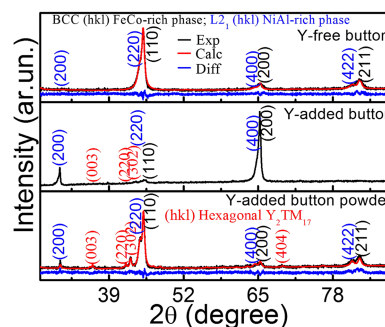


FIG. 1. XRD patterns of Y-free buttons, Y-containing buttons, and Y-containing button powders.

and precipitated as the 2:17 phase. The Y-added button powders are isotropic. Therefore, their three strongest diffraction peaks are from (110), (211), and (200), respectively. The Y-free button has the same three strongest diffraction peaks, implying an isotropic structure. The (200) diffraction peak from the FeCo-rich phase becomes the strongest for the Y-added button, indicating that Y addition develops a (002) preferred orientation. Some extra diffraction peaks for the Y-added button and button powders were detected, which were indexed as the hexagonal Y_2TM_{17} phase. Intensities of diffraction peaks from the Y_2TM_{17} phase relative to the highly textured alnico button seems to be very low, although they can be detected in Figure 1 at 36.2 degree and around 20~ 42 – 44 degrees. After milling, the ingot crystallites become randomly oriented and the (200) texture is lost. In this scenario, the overall intensities also decreased so that the weaker Y_2TM_{17} reflections also become noticeable.

Figure 2 presents thermomagnetic curves of the Y-free and Y-added buttons solutionized at 1220 °C for one half hour and annealed at 810 °C for 10 minutes followed by draw annealing. The data suggest two ferromagnetic-paramagnetic (FP) transitions for the Y-free button, corresponding to the NiAl-rich phase with $T_c = 354$ K and the FeCo-rich phase with $T_c > 900$ K. An extra FP transition was seen for the Y-added button which is associated with the 2:17 phase with $T_c = 766$ K. This result agrees with the XRD data. The T_c of the pure Y_2Co_{17} is about 1200 K,^{11–13} which is much higher than that of the Y-added button here. This indicates that Ni, Cu, and/or Al may enter the 2:17 phase, causing the decrease of T_c . Y addition almost has no effect on the T_c of the NiAl-rich phase.

Figure 3 shows the HAADF image, element mapping and electron-diffraction patterns of the Y-added button solutionized at 1220 °C for one half hour and annealed in a field of 45 kOe at 810 °C for 10 minutes. The HAADF image and Fe mapping in Figs. 3(a) and (b) is perpendicular to the field direction. Some white grains are embedded in the mosaic structure consisting of the gray/white and gray dots. In the HAADF image, the image contrast is related to the average atomic number of the compound, where the areas with higher contrast have larger average atomic number. It is therefore concluded that the white grain corresponds to the 2:17 regions, which have sizes of about 80 nm. The gray/white area is the FeCo-rich nanorod, whose average diameter is 40 nm, as verified by the Fe mapping. The gray area is the NiAl-rich region.

The e-beam used for Fig. 3 is parallel to the $\langle 002 \rangle$ direction or field direction. The electron-diffraction and simulated patterns in Fig. 3(c) and (d) demonstrate that the FeCo-rich phase has the cubic structure with $a = 2.84$ Å. Some superlattice dots were seen in Fig. 3(g) and (h), implying that the NiAl-rich phase has the L_{21} structure with $a = 5.71$ Å. The HAADF image and Fe mapping in Figs. 3(e) and (f) is parallel to the field direction. The FeCo-rich rods were significantly elongated by the applied field of 45 kOe, with lengths exceeding 900 nm and a mean diameter of 40 nm. The rods' aspect ratio is therefore larger than 20, which is beneficial for obtaining a high shape-anisotropy field. The 80 nm 2:17 grains were found to precipitate partially in the FeCo-rich nanorod. Some branching exists in the FeCo-rich nanorods, which was also observed by other researchers.⁴

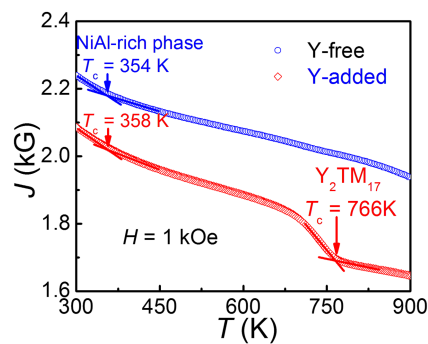


FIG. 2. Temperature dependence of the magnetization of the Y-free and Y-added buttons solutionized at 1220 °C for half an hour and annealed at 810 °C for 10 minutes followed by draw annealing.

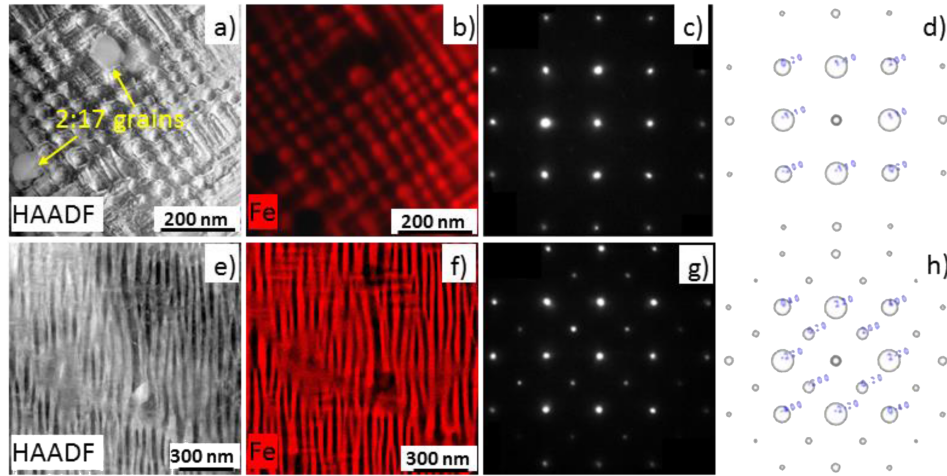


FIG. 3. HAADF imaging of Y-added button solutionized at 1220 °C for half an hour and annealed in a field of 45 kOe at 810 °C for 10 minutes: (a) image perpendicular to applied field direction, (b) corresponding Fe mapping, (c-d) electron diffraction and simulated patterns of the FeCo-rich phase, (e) image parallel to field direction, (f) Fe mapping corresponding to (e), and (g-h) electron diffraction and simulated patterns of the NiAl-rich phase.

Figure 4(a) shows $J(H)$ curves for the Y-added button annealed in different fields at 810 °C for 10 minutes. The applied field appears to enhance the degree of preferred orientation of the FeCo-rich nanods, improving the remanence ratio increases from 0.55 in 0 kOe to 0.80 in 30 kOe. The coercivity increases with applied field due to the enhancement of the shape anisotropy field. Figure 4(b) displays the $J(H)$ curves for the Y-free and Y-added button annealed in a field of 45 kOe at 810 °C for 10 minutes. Y addition develops the (200) texture shown in Fig. 1, enhancing the remanence ratio

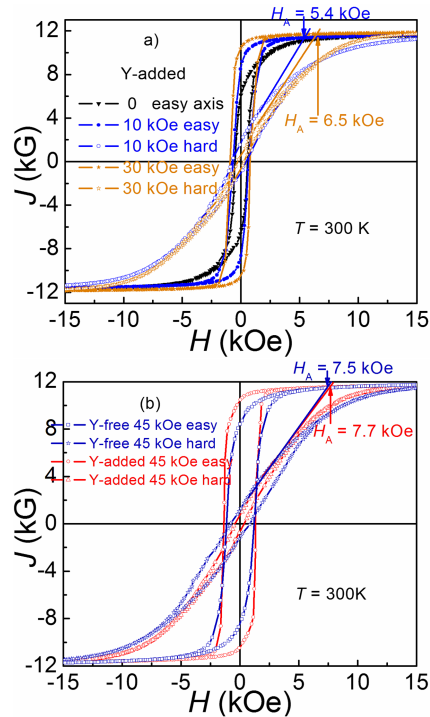


FIG. 4. Hysteresis loops for buttons annealed at 810 °C for 10 minutes: (a) Y-containing buttons annealed in different fields and (b) Y-free and Y-containing buttons annealed in a field of 45 kOe.

up to 0.90 and improving the squareness of the hysteresis loops. Y addition also increases coercivity from 1.1 kOe for the Y-free to 1.3 kOe for the Y-added sample. The respective anisotropy fields for the Y-free and Y-added buttons, 7.5 and 7.7 kOe, are almost the same. We therefore conclude that the increase of coercivity mainly arises from the introduction of the hard hexagonal 2:17 phase. Figure 3 shows that the 2:17 nanograins touch the FeCo-rich rods, which is sufficient to realize exchange coupling. A certain amount of the FeCo-rich nanorods are exchange hardened by contact with the distributed 2:17 nanograins, which also act as the pinning center and impede the movement of domain walls. The above two factors lead to the enhancement of coercivity. When we replaced Y by Sm, the coercivity was increased up to 1.7 kOe (not shown here). This is due to stronger magnetocrystalline anisotropy energy of the $\text{Sm}_2\text{Co}_{17}$ phase than that of the Y_2Co_{17} phase. We have also made alnico 9/SmCo₅ (20 wt%) nanocomposites, whose coercivity is 2.5 kOe (not shown here). The above results indicate that the introduction of high-anisotropy nanograins is a novel and feasible approach to substantially increase the coercivity of alnico magnets. Due to the development of the (002) texture and the formation of the high-anisotropy 2:17 phase, Y addition significantly increases the energy product, from 4.4 MGOe for Y-free to 7.3 MGOe for Y-added.

In summary, we have investigated the influence of Y addition on structure and magnetic properties of alnico 9 buttons. The Y addition leads to a $\langle 200 \rangle$ texture, which helps to increase the remanence ratio and improve the squareness of demagnetization curves. It also induces the formation of high-anisotropy 80 nm 2:17 grains, leading to an increase of coercivity. Finally, a high energy product of 7.3 MGOe has been achieved for the Y-added button. Higher annealing field leads to better alignment of the FeCo-rich nanorods and higher remanence ratios. The introduction of high anisotropy nanograins brings new hopes for developing high-performance alnico magnets for energy applications.

This work was supported by DOE-EERE-VT-PEEM and Propulsion Materials Programs at the Ames Laboratory. Ames Laboratory is operated for the U.S. DOE by Iowa State University under contract no. DE-AC02-07CH11358. The research was performed in part in the Nebraska Nanoscale Facility: National Nanotechnology Coordinated Infrastructure and in the Nebraska Center for Materials and Nanoscience, which are supported by the National Science Foundation under Award ECCS: 1542182 and by the Nebraska Research Initiative.

- ¹ I. E. Anderson, A. G. Kassen, E. M. H. White, A. Palasyuk, L. Zhou, W. Tang, and M. J. Kramer, *AIP Advances* **7**, 056209 (2017).
- ² I. E. Anderson, A. G. Kassen, E. M. H. White, L. Zhou, W. Tang, A. Palasyuk, K. W. Dennis, R. W. McCallum, and M. J. Kramer, *J. Appl. Phys.* **117**, 17D138 (2015).
- ³ P. Lu, L. Zhou, M. J. Kramer, and D. J. Smith, *Sci. Rep.* **4**, 3945 (2014).
- ⁴ L. Zhou, M. K. Miller, P. Lu, L. Q. Ke, R. Skomski, H. Dillon, Q. Xing, A. Palasyuk, M. R. McCartney, D. J. Smith, S. Constantinides, R. W. McCallum, I. E. Anderson, V. Antropov, and M. J. Kramer, *Acta Mater.* **74**, 224 (2014).
- ⁵ W. Y. Zhang, R. Skomski, A. Kashyap, S. Valloppilly, X. Z. Li, J. E. Shield, and D. J. Sellmyer, *AIP Adv.* **6**, 056001 (2016).
- ⁶ A. G. Kassen, E. M. H. White, W. Tang, L. F. Hu, A. Palasyuk, L. Zhou, and I. E. Anderson, *JOM* **69**, 1706 (2017).
- ⁷ W. Tang, L. Zhou, A. G. Kassen, A. Palasyuk, E. M. H. White, K. W. Dennis, M. J. Kramer, R. W. McCallum, and I. E. Anderson, *IEEE Trans. Mag.* **51**, 2101903 (2015).
- ⁸ X. Z. Li, *Microsc. Microanal.* **18**(S2), 1262 (2012).
- ⁹ X. Z. Li, *Microsc. Microanal.* **22**(S3), 564 (2016).
- ¹⁰ S. J. Hu, X. Z. Wei, D. C. Zeng, Z. Y. Liu, E. Brück, J. C. P. Klaasse, F. R. de Boer, and K. H. J. Buschow, *Physica B* **270**, 157 (1999).
- ¹¹ N. Vityk, W. Suski, R. Gladyshevskii, and K. Wochowski, *J Alloys Compd* **442**, 341 (2007).
- ¹² H. Fujii, M. Akayama, K. Nakao, and K. Tatami, *J. Alloys Compd* **219**, 10 (1995).
- ¹³ Z. D. Zhang, C. H. de Groot, E. Brück, F. R. de Boer, and K. H. J. Buschow, *J Alloys Compd* **259**, 42 (1997).